

**CEBELCOR**

RT.323  
RAPPORTS TECHNIQUES CEBELCOR

March 2001

**POTENTIAL-pH DIAGRAMS  
RELEVANT TO 13 Cr STAINLESS STEELS  
IN CHLORIDE AND SULFIDE  
CONTAINING SOLUTIONS**

Reproduction is free, provided reference is made as indicated in the frame above.

CEBELCOR  
Belgian Centre for Corrosion Study  
Avenue des Petits-Champs 4A, B 1410 Waterloo, Belgium  
[www.cebelcor.org](http://www.cebelcor.org)

## POTENTIAL-pH DIAGRAMS RELEVANT TO 13 Cr STAINLESS STEELS IN CHLORIDE AND SULFIDE CONTAINING SOLUTIONS

**L. X. Yang**

School of Metallurgy and Materials, The University of Birmingham,  
Birmingham B15 2TT, UK

**X. Z. Yang**

Department of Chemical Engineering, Shandong University of Technology  
Jinan, P. R. China

**A. Pourbaix**

Belgian Center for Corrosion Study CEBELCOR  
Avenue Paul Héger, grille 2 B1000, Brussels, Belgium

### ABSTRACT

Potential-pH equilibrium diagrams (Pourbaix diagrams) for the systems Fe-Cr-Cl-H<sub>2</sub>O and Fe-Cr-S-H<sub>2</sub>O at 25°C are presented. The mixed oxide FeCr<sub>2</sub>O<sub>4</sub> and the various iron sulphides are considered. The data were selected to provide some consistency between data from different sources. The diagrams are presented for a chloride concentration that corresponds to seawater and for a sulphide concentration of 0.001 mol/kg H<sub>2</sub>S (approximately  $p_{\text{H}_2\text{S}} = 0.01$  bar). The diagrams show the intricate stability regions of iron sulphides, chromium oxide or mixed Fe-Cr oxide and dissolved species within a rather narrow range of potential and acid pH. Some observed facts are reported that illustrate the interest of the diagrams to interpret and predict phenomena. Interesting progress on testing procedures and on mechanisms of localised corrosion could be gained by future work.

Key words : thermodynamics; Pourbaix diagram; 13Cr stainless steel, H<sub>2</sub>S media.

### INTRODUCTION

13Cr and higher alloyed (duplex, superduplex and austenitic) stainless steels show interesting properties to resist corrosion in chloride and sulfide-containing solutions. Nevertheless, there are limits

to their use in these environments. It is well known that in some conditions, oxide can form and in other conditions, black sulfide deposits are observed.

Potential-pH equilibrium diagrams may contribute to identify the conditions for the stability of oxides and sulfides. This may be of interest to understand the mechanisms of various types of corrosion of these alloys in these complex environments.

The results of calculations of the thermodynamic stability of a series of compounds between Fe, Cr, H<sub>2</sub>S and Cl are presented. The conditions selected in this work relate to applications in the offshore oil exploitation.

## SUBSTANCES CONSIDERED AND THEIR STANDARD FREE ENERGIES OF FORMATION

The method for constructing potential-pH diagrams is described in detail by M. Pourbaix<sup>1</sup>. The thermodynamic data used in this work for the binary systems Fe-H<sub>2</sub>O, Cr-H<sub>2</sub>O and Cl-H<sub>2</sub>O come from<sup>1</sup>. The data used for the ternary system Fe-Cl-H<sub>2</sub>O and Cr-Cl-H<sub>2</sub>O come from<sup>2</sup> and<sup>3</sup>, respectively. Diagrams for the three-component systems Fe-S-H<sub>2</sub>O and Cr-S-H<sub>2</sub>O were published<sup>4,5</sup>. For the sake of consistency, we have reconstructed some three-component diagrams using a common set of data. The selected data are listed in Table 1. The data for the other species come from<sup>1</sup>.

The mixed oxide FeCr<sub>2</sub>O<sub>4</sub> is considered as one possible constituent of a passive film of 13Cr stainless steels. Its composition could fit with the spinel structure FeFe<sub>(2-x)</sub>Cr<sub>x</sub>O<sub>4</sub><sup>6</sup>. FeCr<sub>2</sub>O<sub>4</sub>, so-called iron(II) chromite, is a cubic spinel with 8.372 Å of side length<sup>7</sup>. Its standard free energy of formation is slightly different according to different references<sup>8-10</sup>: -313815, -325000 or -348564 cal/mol. More recently, Ball and Nordstrom<sup>11</sup> reviewed published thermodynamic data for chromium oxides and recommended the value of  $-321113 \pm 0.45\%$  cal/mol for FeCr<sub>2</sub>O<sub>4</sub>. In the present study, the most positive value -313815 cal/mol, is chosen to provide a reasonable estimate of the domain of FeCr<sub>2</sub>O<sub>4</sub>.

Two chromium sulfides were considered: CrS and CrS<sub>1.17</sub>. The activities of dissolved sulfide is considered here as 0.001 mol/kg for HS<sup>-</sup> (or approximately  $p_{\text{H}_2\text{S}} = 0.01$  bar), to fit with some oilfield environments<sup>12,13</sup>. Under this sulfide concentration, none of CrS or CrS<sub>1.17</sub> is stable. Therefore, the diagram for the Cr-S-H<sub>2</sub>O system can be obtained by superposing the diagrams for Cr-H<sub>2</sub>O and for S-H<sub>2</sub>O.

Four iron sulfide were considered: FeS<sub>0.93</sub>, FeS, FeS<sub>1.14</sub> and FeS<sub>2</sub>. It is found that the stable regions of FeS<sub>0.93</sub> and FeS are fully covered by that of FeS<sub>1.14</sub>. For simplicity only FeS<sub>1.14</sub> and FeS<sub>2</sub> are chosen here for the Fe-S-H<sub>2</sub>O diagram.

## EQUATIONS AND EQUILIBRIUM FORMULAE

The main reactions considered and their equilibrium conditions calculated for 25°C are listed in Appendix 1.

The potentials are expressed in volts and refer to the standard hydrogen electrode. The activity of water is taken as unity. It is assumed that the solution behaves ideally, so that the dimensionless activity is equal to the numerical value of the molality expressed in moles per kilogram of water<sup>14</sup>.

## EQUILIBRIUM DIAGRAMS AND DISCUSSION

For the diagrams presented, the concentration of all dissolved species is assumed to be  $10^{-6}$  mol/kg except for 0.53 mol/kg for Cl<sup>-</sup> ion, which corresponds to seawater and for 0.001 mol/kg HS<sup>-</sup> (or for H<sub>2</sub>S, S<sup>2-</sup>, SO<sub>4</sub><sup>2-</sup> and HSO<sub>4</sub><sup>-</sup>), thus 0.0005 for S<sub>2</sub>O<sub>3</sub><sup>2-</sup> and 0.00025 for S<sub>7</sub>O<sub>6</sub><sup>2-</sup>. Figure 1 is a E-pH diagram for the system Fe-Cr-Cl-H<sub>2</sub>O where mixed oxide FeCr<sub>2</sub>O<sub>4</sub> is considered.

Whether Cr<sub>2</sub>O<sub>3</sub> will predominate versus FeCr<sub>2</sub>O<sub>4</sub> for 13Cr steels remains to be verified. If this were true, the stability domain of Cr<sub>2</sub>O<sub>3</sub> would derive almost exactly from Figure 2, which shows a diagram for the system Cr-Cl-H<sub>2</sub>O. The difference between Figures 1 and 2, in conditions relevant to oil and gas environments, is that the stability domain of FeCr<sub>2</sub>O<sub>4</sub> is limited to pH slightly higher than that of Cr<sub>2</sub>O<sub>3</sub>. In the presence of acid solution, Fe-Cr alloys tend to corrode with formation of Cr<sup>3+</sup> and FeCl<sup>+</sup> and with evolution of hydrogen.

Figure 3 is a E-pH diagram for the system Fe-Cr-S-H<sub>2</sub>O where two iron sulfides (FeS<sub>1.14</sub> and FeS<sub>2</sub>) and FeCr<sub>2</sub>O<sub>4</sub> are considered. For simplicity, only reactions related to FeCr<sub>2</sub>O<sub>4</sub> are indexed in Figures 1 and 3.

It is observed in Figure 3 that, for the conditions considered ( $[S] = 10^{-3}$  and  $[Fe] = 10^{-6}$ ), the iron sulfide FeS<sub>1.14</sub> is stable in a wide pH range, and particularly at pH lower than those where FeCr<sub>2</sub>O<sub>4</sub> and Cr<sub>2</sub>O<sub>3</sub> are stable. No chromium sulfide is stable in these conditions.

FeS<sub>2</sub> is stable in a wide pH range and at higher potentials. Figure 3 shows that FeS<sub>2</sub> is stable above the hydrogen line (a); thus, FeS<sub>2</sub> would not form when the only oxidizer present is water. Sulfur has a marked effect on Fe-Cr alloys both by introducing a small domain of stability of condensed ferrous sulfide in low pH and low potential conditions, and by decreasing markedly the stability domain of FeCr<sub>2</sub>O<sub>4</sub> to the benefit of ferrous sulfide and pyrite.

Such diagrams are interesting in practice : it is recognized that, when testing 13Cr steels in the solutions defined in EFC 17, NACE TM 0175 or TM 0177, the sample surface either remains bright for some time or turns black. It is considered that cracking initiation is closely related to the black condition. From the diagrams presented here, it is obvious that the two aspects correspond to different electrochemical conditions. The meaning and the reproducibility of the tests would certainly benefit from a better control of these conditions.

Peculiar localised corrosion morphologies were observed on mirror polished 13% Cr stainless steel in deaerated NaCl 30 g/l under 1 bar H<sub>2</sub>S. The stabilized pH and the zero-current potential and pH correspond to the stability of FeS<sub>1.14</sub>. The samples showed some small circular unattacked zones, bright and with the initial mirror polish. In the center of each one of these zones, there is one small pit. These unattacked bright zones are surrounded by rather large corroded areas filled with loose black corrosion products. These corroded areas are in turn surrounded by uncorroded surfaces, covered with a dull or iridescent film. This complex morphology was described as « pits on islands in a lake »<sup>15,16</sup>. Figure 4 shows a cross section through the different zones. With time, the « lakes » (the corroded zones with corrosion products) extend but the bright « islands » remain unattacked. Similar localised corrosion morphologies were observed under 0.1 bar H<sub>2</sub>S and also in a natural gas storage plant with  $p_{H_2S} = 0.016$  bar and  $p_{CO_2} = 0.25$  bar at 50°C, with 60 to 120 g/l Cl<sup>-</sup> in the formation water.

These observations and the E-pH diagrams suggest that the bright uncorroded surfaces are covered with chromium oxide. The pits may provide sacrificial protection to this oxide. The rest of the surface is controlled by the stability conditions of iron sulfide: Figure 3 shows that slight potential and pH variations may lead either to the formation of both chromium oxide and iron sulfide, or to the formation of iron sulfide only, or to corrosion. Such phenomena are indeed observed simultaneously on the sample shown in Figure 4. Stability diagrams may indicate how to favour one or another situation.

## CONCLUSIONS

Potential-pH equilibrium diagrams form a firm basis for the understanding and prediction of corrosion behaviour.

Tentative stability diagrams are presented here for the systems Fe-Cr-Cl-H<sub>2</sub>O and Fe-Cr-S-H<sub>2</sub>O at 25°C, for 0.001 mole/kg HS<sup>-</sup>, or approximately 0.01 bar p<sub>H2S</sub>. Several improvements could be brought to these diagrams, for example by identifying the compounds observed in practice and by using validated data for these compounds. Nevertheless, the diagrams presented are indicative of the behaviour of 13Cr in sour and chloride containing solutions. They have some interest for the sour environments of the oil and gas industry.

The diagram presented in Figure 3 shows that ferrous sulfide, Cr<sub>2</sub>O<sub>3</sub> or FeCr<sub>2</sub>O<sub>4</sub> and Fe<sup>2+</sup> and Cr<sup>3+</sup> are stable all within a very narrow potential and pH range. It is felt that observations from the practice can find an explanation from such diagrams and that actions to favour one or another behaviour can be derived from them.

More representative and more reproducible or better controlled testing procedures can be derived from such diagrams. The study of mechanisms of localised corrosion in H<sub>2</sub>S + Cl<sup>-</sup> environment, without oxygen, should benefit from such theoretical background. More work is needed to improve the quality and the applicability of such data to practical problems.

## ACKNOWLEDGEMENT

Helpful discussions with Dr. J.P.G. Farr are gratefully acknowledged.

## REFERENCES

1. M. Pourbaix, Atlas of Electrochemical Equilibrium in Aqueous Solutions (NACE, Cebelcor, 1974).
2. M. Pourbaix, A. Pourbaix and X. Z. Yang, « Chemical Aspects of Denting in Steam Generators », EPRI n°NP-2177, December 1981.
3. B. C. Syrett, D. D. Macdonald, H. Shih and S. S. Wing, « Corrosion Chemistry of Geothermal Brines », S.R.I., USA, 1977.
4. A. K. Singh and A. Pourbaix, « E-pH Diagrams for the System Fe-S-H<sub>2</sub>O from 25°C to 150°C », Rapp. Techniques CEBELCOR, 166, RT.318 (1997).
5. C. M. Chen, K. Aral, and G. J. Theus, « Computer-Calculated Potential pH Diagrams to 300°C », EPRI Report NP-3137, Vol. 2, June 1983.

6. D. Cubicciotti, *J. Nuclear Materials*, 167, (1989), p.241.
7. J.D.H. Donnay and H.M. Ondik, *Crystal Data (inorganic compounds)*, 3<sup>rd</sup> ed., Vol.2 (U.S. Depart. of Commerce, NBS and the Joint Committee on Powder Diffraction Standards, 1973)
8. X. Yang, *The Handbook of Thermodynamics Data in Aqueous Solution at Elevated Temperature*. (Yejin Press, Beijing, 1983).
9. M.Kh. Karapet'yants and M.K. Karapet'yants, *Handbook of Thermodynamic Constants of Inorganic and Organic Compounds*, Transl. by J. Schmorak (Ann Arbor-Humphrey Sc. Publ., London, 1970).
10. Barin, O. Knacke and O. Kubaschewski, *Thermochemical Properties of Inorganic Substances. Supplement* (Springer-Verlag Berlin Heidelberg New York, 1977).
11. J. W. Ball and D.K. Norstrom, *J. Chemical And Engineering Data* 43 (1998), p.895.
12. M. Saenz de Santa Maria and A. Turnbull, *Corrosion Science*, 29 (1989), p.69.
13. G. Firro, G.M. Ingo, F. Mancia, L. Scoppio, N. Zaccetti, *J. Mat. Sci.*, 25 (1990), p.1407.
14. M. Philippe and E. Protopopoff, *J. Electrochem. Soc.* 144 (1997), p.1586.
15. A.Pourbaix. «Morphology of localised corrosion of 13 % Cr steel and carbon steel in H<sub>2</sub>S solutions», *Rapports Techniques CEBELCOR*, 166, RT.316 (1997).
16. A.Pourbaix, M.Amalhay, A.Singh «Contribution to the mechanisms of localised corrosion of C-steel and 13Cr stainless steel in H<sub>2</sub>S environments», *Eurocorr'97, Trondheim*, vol.1 (1997), p.213-218.
17. W.M.Latimer, « The oxidation states of the elements and their potentials in aqueous solutions » (New-York, Prentice Hall, Inc. 1952).

TABLE 1 : STANDARD GIBBS FREE ENERGIES OF FORMATION OF SOME SPECIES CONSIDERED (data for the other species considered come from <sup>1)</sup>)

Species	$\Delta G_f^\circ$ (298.15 K) cal/mol		
	This paper	Other sources	
FeCl <sup>+</sup>	-53800	-53797 <sup>2</sup>	-53800 <sup>8</sup>
FeCl <sub>2</sub> <sup>+</sup>	-69694	-69700 <sup>2</sup>	-69694 <sup>8</sup>
FeCr <sub>2</sub> O <sub>4</sub>	-313815	-325000 <sup>17</sup>	-348564 <sup>10</sup> -313815 <sup>8</sup>
CrCl <sup>3+</sup>	-80903		-80903 <sup>8</sup>
Cl <sup>-</sup>	-31405	-31372 <sup>2</sup>	-31350 <sup>17</sup> -31405 <sup>8</sup>
FeS <sub>0.93</sub>	-22300		-22300 <sup>3</sup>
FeS	-24368		-24368 <sup>3</sup> -24092 <sup>8</sup>
FeS <sub>1.14</sub>	-29123		-29123 <sup>3</sup>
FeS <sub>2</sub>	-38256		-38256 <sup>3</sup> -38289 <sup>8</sup>
CrS	-37811		-37811 <sup>10</sup>
CrS <sub>1.17</sub>	-40128		-40128 <sup>10</sup>

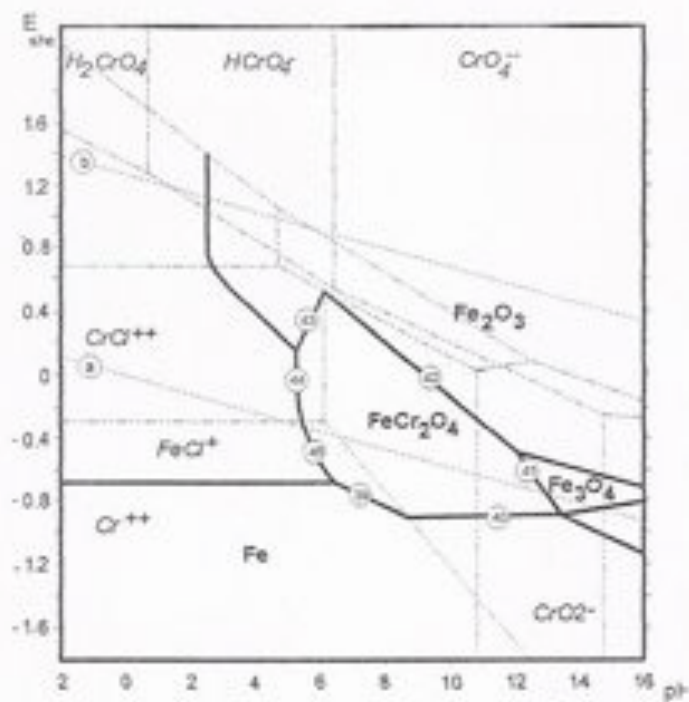


FIGURE 1: Potential-pH equilibrium diagram for the system Fe-Cr-Cl-H<sub>2</sub>O at 25°C, considering FeCr<sub>2</sub>O<sub>4</sub>

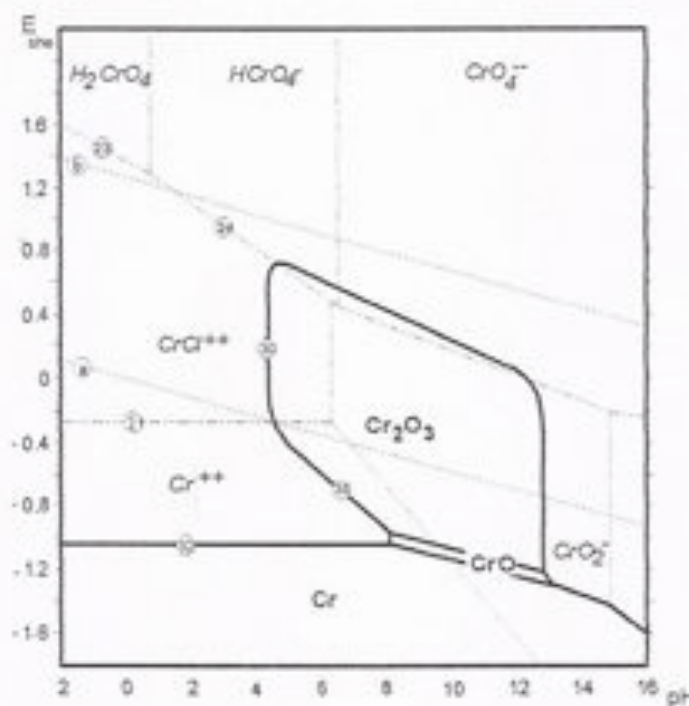


FIGURE 2 : Potential-pH diagram for the system Cr-Cl-H<sub>2</sub>O at 25°C

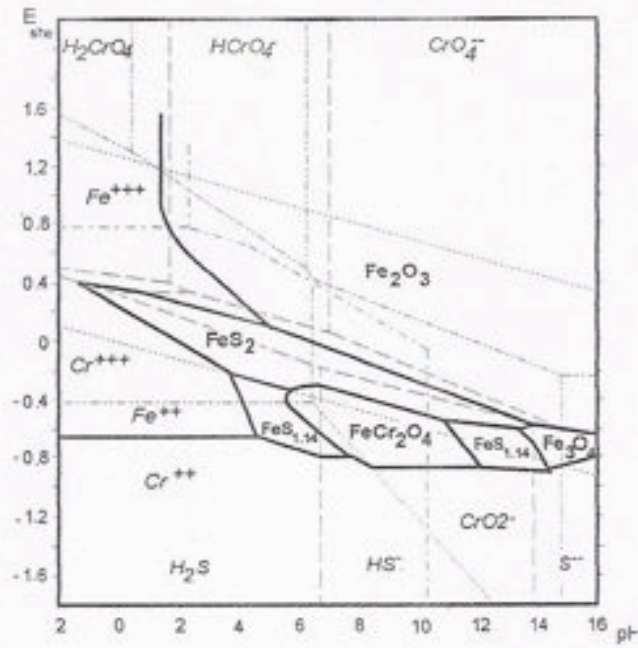


FIGURE 3 : Potential-pH equilibrium diagram for the system Fe-Cr-S-H<sub>2</sub>O at 25°C, considering FeS<sub>1.17</sub> and FeCr<sub>2</sub>O<sub>4</sub>



FIGURE 4 : Cross section of localised corrosion of 13Cr steel in NaCl 30 g/l and 1 bar H<sub>2</sub>S

APPENDIX 1. REACTIONS AND EQUILIBRIUM CONDITIONS AT 25°C

Only the reactions and equilibrium equations for the major lines of Figures 1, 2 and 3 are listed below. The other lines are reported in references <sup>3-5</sup>.

For Figure 1 : System Fe-Cr-Cl-H<sub>2</sub>O

39.  $Fe + 2Cr^{3+} + 4H_2O = FeCr_2O_4 + 8H^+ + 4e^-$   
 $E^0 = -0.031 - 0.1182pH - 0.0295\log(Cr^{3+})$
40.  $Fe + 2CrO_2 = FeCr_2O_4 + 2e^-$   
 $E^0 = -1.250 - 0.0591\log(CrO_2)$
41.  $3FeCr_2O_4 + H_2O = Fe_3O_4 + 6CrO_2 + 8H^+ + 2e^-$   
 $pH = 3.410 - 0.2364pH + 0.1773\log(CrO_2)$
42.  $2FeCr_2O_4 + 3H_2O = Fe_2O_3 + 4CrO_2 + 6H^+ + 2e^-$   
 $E^0 = 2.347 - 0.1773pH + 0.1182\log(CrO_2)$
43.  $2FeCr_2O_4 + 4Cl^- + 10H^+ = Fe_2O_3 + 4CrCl_2 + 5H_2O + 2e^-$   
 $E^0 = -0.670 + 0.2955pH - 0.1182\log(Cl^-) + 0.1182\log(CrCl_2)$
44.  $2CrCl_2 + FeCl_2 + 4H_2O = FeCr_2O_4 + 3Cl^- + 8H^+$   
 $pH = 3.15 + 3/8\log(Cl^-) - 1/8\log((CrCl_2)^2/(FeCl_2))$
45.  $2Cr^{3+} + FeCl_2 + 4H_2O = FeCr_2O_4 + Cl^- + 8H^+ + 2e^-$   
 $E^0 = 0.424 - 0.2364pH + 0.0295\log(Cl^-) - 0.0295\log((Cr^{3+})^2/(FeCl_2))$

For Figure 2 : System Cr-Cl-H<sub>2</sub>O

21.  $Cr^{3+} + Cl^- = CrCl^{2+} + e^-$   
 $E^0 = -0.321 - 0.0591\log(Cl^-) + 0.0591\log(CrCl^{2+})/(Cr^{3+})$
23.  $CrCl^{2+} + 4H_2O = H_2CrO_4 + 6H^+ + Cl^- + 3e^-$   
 $E^0 = 1.306 - 0.1182pH + 0.0197\log(Cl^-) + 0.0197\log(H_2CrO_4)/(CrCl^{2+})$
24.  $CrCl^{2+} + 4H_2O = HCrO_4^- + 7H^+ + Cl^- + 3e^-$   
 $E^0 = 1.321 - 0.1379pH + 0.0197\log(Cl^-) + 0.0197\log(HCrO_4^-)/(CrCl^{2+})$
30.  $2CrCl^{2+} + 3H_2O = Cr_2O_3 + 6H^+ + 2Cl^-$   
 $pH = 2.31 + 1/3\log(Cl^-) - 1/3\log(CrCl^{2+})$

For Figure 3 : System Fe-Cr-S-H<sub>2</sub>O

70.  $Fe + 2Cr^{3+} + 4H_2O = FeCr_2O_4 + 8H^+ + 4e^-$   
 $E^0 = -0.031 - 0.1182pH - 0.0295\log(Cr^{3+})$
71.  $Fe + 2CrO_2 = FeCr_2O_4 + 2e^-$   
 $E^0 = -1.250 - 0.0591\log(CrO_2)$
72.  $FeCr_2O_4 + 1.14HS + 5.72H^+ = FeS_{134} + 2Cr^{3+} + 4H_2O + 0.28e^-$   
 $E^0 = -5.825 + 1.2073pH + 0.4221\log(Cr^{3+}) - 0.2406\log(H_2S)$
73.  $FeCr_2O_4 + 1.14HS = FeS_{134} + 2CrO_2 + 1.14H^+ + 0.28e^-$   
 $E^0 = 3.884 - 0.2406pH + 0.4221\log(CrO_2) - 0.2406\log(HS)$
74.  $FeS_{134} + 2Cr^{3+} + 4H_2O = FeCr_2O_4 + 1.14HS + 5.72H^+ + 1.72e^-$   
 $E^0 = 0.474 - 0.1963pH + 0.0392\log(H_2S) - 0.0687\log(Cr^{3+})$
75.  $FeS_{134} + 2Cr^{3+} + 4H_2O = FeCr_2O_4 + 1.14HS + 6.86H^+ + 1.72e^-$   
 $E^0 = 0.749 - 0.2357pH + 0.0392\log(HS) - 0.0687\log(Cr^{3+})$
76.  $FeCr_2O_4 + 2HS + 4H^+ = FeS_2 + 2Cr^{3+} + 4H_2O + 2e^-$   
 $E^0 = -0.892 + 0.1182pH - 0.0591\log(Cr^{3+}) - 0.0591\log(H_2S)$
77.  $FeCr_2O_4 + 2HS = FeS_2 + 2CrO_2 + 2H^+ + 2e^-$   
 $E^0 = 0.290 - 0.0591pH + 0.0591\log(CrO_2) - 0.0591\log(HS)$